Rare Met. (2015) 34(3):160–163
DOI 10.1007/s12598-014-0444-7

RARE METALS
www.editorialmanager.com/rmet

# Microstructure and phase compositions of as-cast Mg–3.9Zn–0.6RE (Gd, Y) alloy with different Gd/Y ratios

**Yang Yang, Kui Zhang*, Ming-Long Ma, Jia-Wei Yuan**

Received: 25 February 2014 / Revised: 8 May 2014 / Accepted: 30 December 2014 / Published online: 29 January 2015


**Abstract** Mg–Zn–RE (Gd, Y) alloys with different Gd/Y atomic ratios were prepared by conventional casting, and the microstructure of the alloys was studied by multiple means. Icosahedral quasicrystal phases are observed in all alloys. The different Gd/Y atomic ratios affect the microstructures of the alloys irregularly. The alloy with more Gd has large dendritic structure and more complicated phase composition which are composed of I-phase lamellar eutectic, W-phase divorced eutectic, Mg–RE cuboid particles and Mg–Zn binary phases. Other two alloys show similar microstructures and phase compositions with very thin lamellar eutectics which distribute along the interdendritic region, and the lamellar eutectics are formed by I-phase and Mg. The element contents of the I-phases and Mg–RE phases are partially controlled by the Gd/Y atomic ratio.

**Keywords** Mg–Zn–RE alloy; Icosahedral quasicrystalline; Microstructure; Atomic ratio

## 1 Introduction

Since the icosahedral quasicrystalline (IQC) was discovered and confirmed by Shechtman in a rapidly solidified Al–Mn alloy, many alloy systems containing IQC were built, including Mg–Zn–RE system [1–7]. The IQC phases (I-phases) have many attractive properties, such as high hardness, high thermodynamic stability and low interfacial energy due to its special crystal structure [8]. In magnesium alloy, I-phases could be prepared by conventional casting in Mg–Zn–RE alloys, which indicates that the I-phase will have more potential applications in the development of magnesium alloys.

In the last decade, Mg–Zn–RE alloy systems were greatly improved, especially Mg–Zn–Y and Mg–Zn–Gd alloy systems [9–12]. Generally, the interface between the quasicrystalline phase and the matrix is more stable and has low lattice mismatching which leads to good properties for the alloy. By strengthening the effect of I-phases, the mechanical properties of those alloys are greatly enhanced. Magnesium alloys reinforced with I-phases show high strength and good ductility as well as remarkable deformation ability. Researches show that the Mg93Zn6Y1 alloy with chill casting and direct extruded processes has excellent properties with tensile strength of 416 MPa, elongation of 16 % and grain size of 1 μm [13]. The Mg–Zn–Gd alloys have I-phase type which also exists in Mg–Zn–Y alloys. It means that the formation of IQC is decided by the alloy system rather than the specific element [12, 14–17]. But the experimental data of the addition of Gd and Y elements to the Mg–Zn alloy at the same time are limited, especially the effect of Gd/Y ratio on the microstructure of the alloy. In the present work, the microstructure of Mg–3.9Zn–0.6RE (at%) alloys with different Gd/Y ratios was studied. The main aim of the present paper is to study the effect of the Gd/Y ratio on the microstructure and the composition of the phases, which can develop the data of the IQC magnesium alloy.

## 2 Experimental

The alloys with the nominal composition in Table 1 were prepared by melting high-purity elements in electromagnetic

Y. Yang, K. Zhang*, M.-L. Ma, J.-W. Yuan
State Key Laboratory for Fabrication and Processing of Nonferrous Metals, General Research Institute for Nonferrous Metals, Beijing 100012, China
e-mail: arietta@163.com

**Table 1** Nominal and measured compositions of experimental alloys

| Alloys | Nominal composition/at% | | | Measured composition/at% | | |
|---|---|---|---|---|---|---|
| | Zn | Gd | Y | Zn | Gd | Y |
| ZEW930 | 3.90 | 0.45 | 0.15 | 3.91 | 0.48 | 0.14 |
| ZEW921 | 3.90 | 0.30 | 0.30 | 3.93 | 0.29 | 0.23 |
| ZEW912 | 3.90 | 0.15 | 0.45 | 4.07 | 0.16 | 0.42 |

induction furnace protected by $SF_6/CO_2$ protective gas. After melting at 780 °C for 10 min and holding for 10 min at 750 °C, the melt with the crucibles was directly chilled in water. The ingots were 350 mm in height and 50 mm in diameter. All specimens were obtained from the top of the ingots. The microstructures of the specimens were observed by scanning electron microscopy (SEM, CarlZeiss EVO1) with energy-dispersive spectrometer (EDS) and optical microscopy (OM), and the phases were identified by X-ray diffraction (XRD, X'pert PRO MPD) and differential scanning calorimetry (DSC, NETZSCH DSC404F3).

## 3 Results and discussion

According to the result of the calculation of the phase diagram, the Zn/RE ratio is a controlling parameter for the phase constituencies. When the Zn/RE ratio is 6, the composition of the alloy should be α-Mg + I-phase in equilibrium [18]. When the Zn/RE ratio is lower than 6, it will be W-phase ($Mg_3Y_2Zn_3$, fcc structure) in the alloy which has no strengthened effect on the alloy, so the appearance of W-phase must be eliminated [19]. When the Zn/RE ratio is larger than 6, MgZn and $MgZn_2$ binary phases will emerge in equilibrium. At the high-temperature region of the ternary phase diagram (about 673 K), the alloy is also composed of α-Mg + I-phase when the Zn/RE ratio is a little larger than 6. Therefore, the nominal compositions of the alloys were designated as Mg–3.9Zn–0.6RE, and Gd and Y were chosen as the rare earth elements in this study. The Gd/Y ratios of the alloys are approximately 3:1, 1:1 and 1:3 and the nominal and measured compositions of the experimental alloys are shown in Table 1, denominated as ZEW930, ZEW921 and ZEW912, respectively. The measured compositions show that the yield of Zn and Gd is higher and the yield of Y is lower, but the Zn/RE atomic ratios are not far from 6, which means that the ingots meet the expectations.

Figure 1 shows the OM images of the as-cast alloy. All of the alloys have dendritic structures with different dendrite spaces. The dendrite spaces of ZEW930, ZEW921 and ZEW912 are 34, 25 and 23 μm, respectively. It can be seen that the microstructure of ZEW930 shows more differences compared with those of ZEW921 and ZEW912. Not only the dendrite space is larger, but also the distributions of the second phases are more diversified. Besides the lamellar phases between the dendrite, particles are observed inside the dendrite and some of the interdendritic regions show gray contrast which may refer to a new composition. Compared with the microstructure of ZEW930, those of ZEW921 and ZEW912 have the same type. In Fig. 1b, c, bulky dendrite arms are clearly observed with few particles inside the grains. Some dendrites fuse and turn into isometric grains. The second phases are mainly distributed at the interdendritic area with the thickness of several microns.

The SEM observations of the as-cast alloys are shown in Fig. 2. It shows that the ZEW930 alloy is composed of four kinds of morphology structures: α-Mg solid solution matrix, lamellar eutectic structure, bulk divorced eutectic and cuboid particle. The thickness of the lamellar eutectic phase shown in Fig. 2a is about 1–2 μm. The size of the bulk divorced eutectic which intergrows with the lamellar eutectic is 10–20 μm. According to the EDS analysis in Table 2, the bulk divorced eutectic marked as Point 1 in Fig. 2a is Mg–Zn–RE ternary phase with the Zn/RE ratio of 7:4, which means it may be the W-phase. Point 2 in Fig. 2b shows a cuboid particle with the size of 3–4 μm. EDS result indicates that the cuboid particle is $MgRE_5$ phase. In the same way, according to the EDS result, the lamellar eutectic marked by Point 3 should be identified as I-phase, as the Zn/RE ratio is 4:1 which is close to the element content of I-phase. In Fig. 2c, d, the second phases

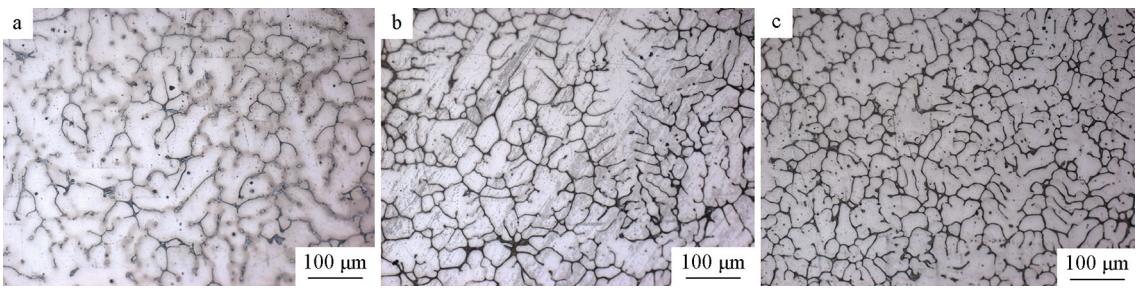


**Fig. 1** OM images of as-cast alloys: **a** ZEW930, **b** ZEW921 and **c** ZEW912

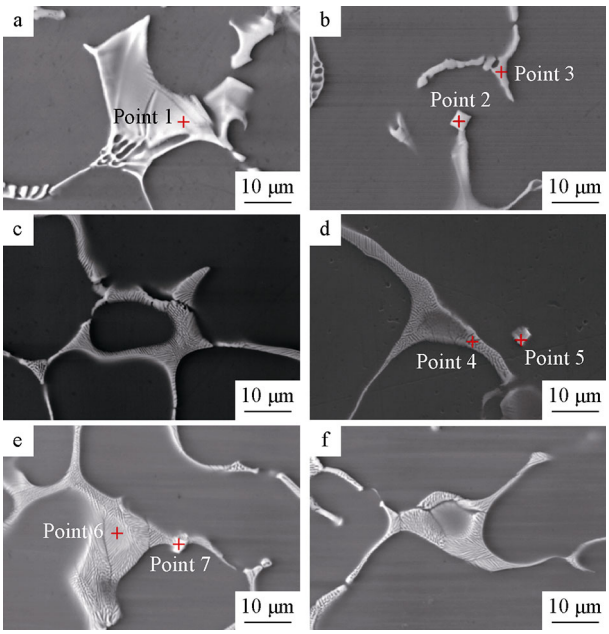


**Fig. 2** SEM images of as-cast alloys: **a**, **b** ZEW930; **c**, **d** ZEW921; **e**, **f** ZEW912

**Table 2** EDS results of points marked in Fig. 2

| Points | Content/at% | | | | Element ratio | |
|---|---|---|---|---|---|---|
| | Mg | Zn | Y | Gd | Zn/RE | Gd/Y |
| 1 | 44.00 | 35.98 | 6.12 | 13.91 | 7:4 | 2:1 |
| 2 | 18.72 | 2.33 | 54.30 | 24.66 | – | 1:2 |
| 3 | 46.55 | 42.26 | 5.21 | 5.98 | 4:1 | 1:1 |
| 4 | 70.24 | 23.74 | 3.48 | 2.54 | 4:1 | 2:3 |
| 5 | 32.34 | 1.41 | 55.24 | 11.00 | – | 1:5 |
| 6 | 75.89 | 20.01 | 3.05 | 1.05 | 5:1 | 1:3 |
| 7 | 28.71 | 3.62 | 60.05 | 7.63 | – | 1:8 |

located at the interdendritic region are clearly observed in the ZEW921 alloy. The slice-shaped second phases observed in OM are actually lamellar eutectics in SEM observation with the thickness of 0.5 μm for each slice. The EDS results show that the lamellar eutectics marked as Point 4 are I-phases and the particle indicated by Point 5 is Mg–RE binary phase. The microstructure of the ZEW912 alloy in Fig. 2e, f is similar to that of the ZEW921 alloy. Very fine lamellar eutectics and cuboid particle marked as Points 6 and 7 in Fig. 2e are identified as I-phase and Mg–RE binary phase, respectively.

In order to confirm the phase composition of the as-cast alloys, the DSC and XRD analyses are presented in Fig. 3. The DSC result shows that there are three endothermic peaks for ZEW930 alloy. The first peak is 350 °C which may refer to the decomposition of Mg–Zn binary phases. But there is no evidence for the appearance of the Mg–Zn phases in the XRD and EDS analysis. This may be because that the Mg–Zn phases in the ZEW930 alloy are too small to be detected by the SEM. Moreover, the characteristic peaks of $Mg_7Zn_3$ are close to the characteristic peaks of W-phase, which means that they may overlap. The next endothermic peak appears at 446 °C which is the reaction temperature of the peritectic reaction [18]:

$$L + W \xleftrightarrow{(448 \pm 2)^{\circ}C} I + Mg \quad (1)$$

Combined with the XRD patterns, the appearance of I-phase in all alloys can be confirmed. The temperature of the third endothermic peak is 501 °C which is the melting temperature of W-phase. Another mismatching between the SEM and the XRD results is the existence of the cuboid Mg–RE phases. These phases are observed in SEM images of all three alloys, but have no characteristic peak in all XRD patterns. It could be due to the low content of the Mg–RE phases which could not be detected by XRD sensor.

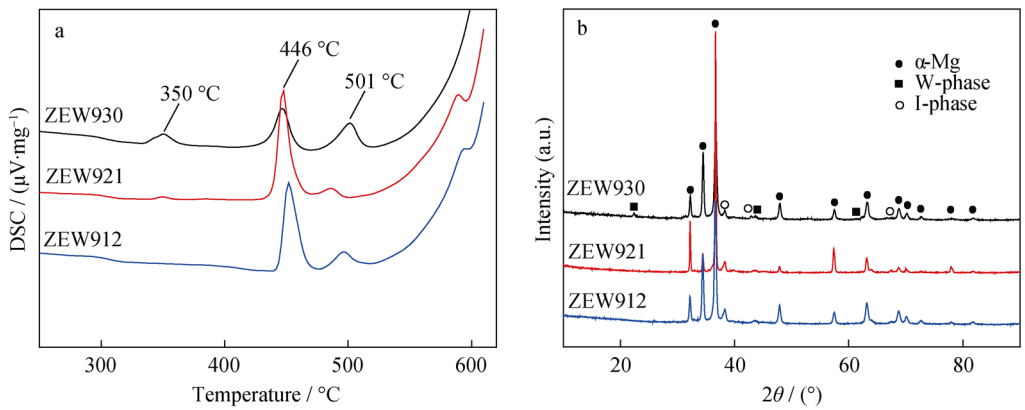


**Fig. 3** Phase analysis of as-cast alloys: **a** DSC curves and **b** XRD patterns

In comprehensive, these ingots with different Gd/Y ratios meet expectations. However, the effect of the Gd/Y ratio is irregular, because the ZEW930 alloy shows significant difference in microstructure and phase composition compared with ZEW921 and ZEW912 alloys. The dendrite arms are much wider, and the $Mg_7Zn_3$ and W-phases are only detected in ZEW930 alloy. The possible reason is that the solid solubility and melting point of Gd and Y are different, for Gd has higher solubility and lower melting point compared with Y. Thus, Gd may first dissolve in the melt and form W-phase. $MgRE_5$ phase with high melting temperature may form at the same time, which may suppress the peritectic reaction and make Zn form Mg–Zn phase. The composition of I-phase can also be affected by Gd/Y ratio. The Gd/Y ratios of the I-phases in ZEW930, ZEW921 and ZEW912 alloys are about 1:1, 2:3 and 1:3, respectively. These trends can also be found in the compositions of the cuboid Mg–RE phases in the three alloys. Y is the primary element of the Mg–RE phases, and the contents of Gd in Mg–RE phases decrease as the Gd/Y ratios of the alloys reduce. Thus, the Gd and Y elements can substitute each other to some extent, but there is no obvious change in the characterization of the phases, as there is no significant difference between the ZEW921 and ZEW912 alloys.

## 4 Conclusion

Three Mg–3.9Zn–0.6RE alloys with different Gd/Y atomic ratios were prepared, and the microstructures and phase compositions were studied. All alloys have dendritic structure, and the dendrite spaces of ZEW930, ZEW921 and ZEW912 are 34, 25 and 23 μm, respectively. The Gd/Y atomic ratio shows irregular effect on the microstructures of the alloys. The ZEW930 alloy with the Gd/Y ratio of 3:1 exhibits more complicated phase compositions as there are I-phase, W-phase, Mg–Zn and Mg–RE binary phases with multiple morphologies. The microstructures and phase compositions of the ZEW921 and ZEW912 alloys are similar, with very thin I-phase lamellar eutectic lying on the interdendritic area and few cuboid Mg–RE particles distributing in the basis. Gd/Y ratio can affect the element contents of the I-phases and Mg–RE phases, and the element contents of the phases have the same change rule as the Gd/Y ratios in the alloys.

**Acknowledgments** This work was financially supported by the National Natural Science Foundation of China (No. 51204020) and the National Basic Research Program of China (Nos. 2013CB632202 and 2013CB632205).

## References

[1] Luo ZP, Zhang SQ. On the stable quasicrystals in slowly cooled Mg–Zn–Y alloys. Scripta Mater. 1994;32(9):1411.
[2] Guo YC, Cheng L, Wu YX. Microstructure and phase analysis of Mg–Gd–Zn alloys. Chin J Rare Met. 2014;38(4):603.
[3] Yuan GY, Yong L, Ding WJ. Effects of extrusion on the microstructure and mechanical properties of Mg–Zn–Gd alloy reinforced with quasicrystalline particles. Mater Sci Eng A. 2008;474(1):348.
[4] Li Y, Peng SH, Yang JJ. Microstructure and properties of Mg–xSn–2Al–1.5Zn–0.8Si ($x = 3, 5, 8$) magnesium alloys. Chin J Rare Met. 2014;38(6):973.
[5] Li T, Zhang K, Li XG, Du ZW, Li YJ, Ma ML, Shi GL. Dynamic precipitation during multi-axial forging of an Mg–7Gd–5Y–1Nd–0.5Zr alloy. J Magn Alloys. 2013;1(1):47.
[6] Jiang QT, Zhang K, Li XG, Li YJ, Ma ML, Shi GL, Yuan JW. The corrosion behaviors of Mg–7Gd–5Y–1Nd–0.5Zr alloy under $(NH_4)_2SO_4$, NaCl and $Ca(NO_3)_2$ salts spray condition. J Magn Alloys. 2013;1(3):230.
[7] Zhang K, Zhang X, Deng X, Li XG, Ma ML. Relationship between extrusion, Y and corrosion behavior of Mg–Y alloy in NaCl aqueous solution. J Magn Alloys. 2013;1(2):134.
[8] Singh A, Somekawa H, Mukai T. High temperature processing of Mg–Zn–Y alloys containing quasicrystal phase for high strength. Mater Sci Eng A. 2011;528(1):6647.
[9] Singh A, Nakamura M, Watanabe M. Quasicrystal strengthened Mg–Zn–Y alloys by extrusion. Scr Mater. 2003;49(1):417.
[10] Wan DQ, Yang GC, Zhu M. Microstructure formation and mechanical property involving icosahedral quasicrystal phase of Y rich Mg–Zn–Y quasicrystal alloy. Acta Metall. 2007;20(6):429.
[11] Yong L, Yuan GY, Ding WJ. Deformation behavior of Mg–Zn–Gd-based alloys reinforced with quasicrystal and Laves phases at elevated temperatures. J Alloys Compd. 2007;427(1):160.
[12] Yong L, Yuan GY, Lu C. Stable icosahedral phase in Mg–Zn–Gd alloy. Scr Mater. 2006;55(1):919.
[13] Singh A, Osawa W, Somekawa H. Ultra-fine grain size and isotropic very high strength by direct extrusion of chill-cast Mg–Zn–Y alloys containing quasicrystal phase. Scr Mater. 2011;64(1):661.
[14] Hua H, Kato H, Yuan GY. The effect of nanoquasicrystals on mechanical properties of as-extruded Mg–Zn–Gd alloy. Mater Lett. 2012;79(1):281.
[15] Yan H, Chen RS, Han EH. Room-temperature ductility and anisotropy of two rolled Mg–Zn–Gd alloys. Mater Sci Eng A. 2010;527(1):3317.
[16] Cai ZX, Jiang HT, Tang D, Ma Z, Kang Q. Texture and stretch formability of rolled Mg–Zn–RE (Y, Ce, and Gd) alloys at room temperature. Rare Met. 2013;32(5):441.
[17] Shi WY, Ma Y. Microstructure of ZM6 Magnesium alloy with different Nd content. Rare Met. 2013;32(3):234.
[18] Shao G, Varisani V, Fan Z. Thermodynamic modelling of the Y–Zn and Mg–Zn–Y systems. Calphad. 2006;30(1):286.
[19] Xu DK, Tang WN, Liu L. Effect of W-phase on the mechanical properties of as-cast Mg–Zn–Y–Zr alloys. J Alloys Compd. 2008;461(1):248.